BIS ENERGY AND ENGINEERING

Volume 1 2024 | DOI: 10.31603/biseeng.84
5th Borobudur International Symposium on Science and Technology (BIS-STE) 2023

UNIMMA PRESS
UNIVERSITAS MUHAMMADIYAH MAGELANG

# Stress analysis and fatigue life prediction of portable rocket motor test stand using finite element method

L A N Wibawa[1*], I Rusyana[1], G Nugraha[1], D Koswara[1], D Muhdiyat[1], Y Kristiyana[1], H Subarkah[1] and D Irawan[1]

[1] National Research and Innovation Agency (BRIN), Jakarta, Indonesia
[*]Corresponding author email: lasinta.ari.nendra.wibawa@brin.go.id

## Abstract

A portable rocket motor test stand serves as the apparatus to evaluate the performance of rocket motors under controlled conditions. This equipment is crucial for assessing the thrust of the RX 200 rocket motor and examining the capabilities of various components, including the tube, propellant, insulator, igniter, nozzle, and rocket cap itself. Before conducting the RX 200 rocket flight test, a preliminary assessment using this equipment is essential. Therefore, the design of a rocket motor test stand must be carefully calculated to ensure that the tool functions as desired. In this study, thrust force variations of 10,000, 12,000, 14,000, and 16,000 N were applied. The portable rocket motor test stand utilized Aluminium 6061-T6, known for its low density, corrosion resistance, and moderate strength. Finite element analysis was conducted using Ansys Workbench software. The results of the fatigue simulation reveal that the portable rocket motor test stand fails to achieve a service life of 1 million cycles at a thrust of 16,000 N.

## Keywords

Stress analysis, life prediction, portable rocket motor, finite element method

## Introduction

The equipment utilized to evaluate the performance of a rocket motor under controlled conditions is known as a rocket motor test stand. This apparatus is employed to measure the thrust generated by the rocket motor and assess the functionality of various components, including the tube, propellant, insulator, igniter, nozzle, and rocket cap. Space agencies, aviation authorities, and certain educational institutions, as indicated by references, utilize this equipment for educational purposes [1-16]. Conducting a pre-flight examination using this apparatus is imperative before launching a rocket flight test. This testing phase plays a crucial role in ensuring that the rocket

**Published:**
October 20, 2024



Selection and Peer-review under the responsibility of the 5th BIS-STE 2023 Committee

propulsion system adheres to the necessary standards for safe and successful operation.

This paper presents the design of a rocket motor test stand, encompassing static stress analysis and fatigue life prediction. The dimensions of the rocket motor test stand are as follows: a length of 1200 mm, a width of 600 mm, a height of 330 mm, and an internal diameter of the test stand measuring 200 mm. Consequently, the maximum diameter of the rocket tube that can be accommodated for testing is 200 mm. The rocket motor test stands are constructed using Aluminium 6061-T6, chosen for its low density, corrosion resistance, and moderate strength.

This study involved variations in thrust, specifically 10,000, 12,000, 14,000, and 16,000 N. Numerical simulations were conducted using Ansys Workbench software and the finite element method. Ansys Workbench is widely recognized for simulating components of rockets and aeroplanes, as highlighted in references [17,18]. Ansys offers several advantages, including its compatibility with a broad range of Computer-Aided Design (CAD) software such as SolidWorks, Catia, Autodesk Inventor, Autodesk Fusion, and Creo Parametric.

# Material and Method

## *Material*

The material selected for the rocket motor test stand is Aluminium 6061-T6, known for its medium tensile strength, good formability, corrosion resistance, and lightweight properties. Widely favoured in the aerospace industry, Aluminium 6061-T6 stands out for its exceptional strength-to-weight ratio, providing sturdy structural support while maintaining a relatively low density. This feature significantly contributes to the overall lightweight design of aerospace vehicles, making it a preferred material for aircraft and rocket components. Its corrosion resistance ensures durability in challenging environmental conditions, which is particularly crucial for extended exposure to diverse elements during flight.

In addition to these qualities, Aluminium 6061-T6 offers excellent machinability, streamlining the manufacturing process and allowing for intricate designs. These characteristics collectively make it an ideal choice for critical components, ensuring that both aircraft and rocket systems benefit from a combination of structural integrity and operational efficiency. Detailed mechanical properties of Aluminium 6061-T6 are presented in Table 1, utilizing data obtained from Ansys software.

Table 1. Mechanical properties of Aluminium 6061-T6 (based on data from Ansys software)

| Material | Density ($g/cm^3$) | Young Modulus (GPa) | Tensile Strength (MPa) | Yield Strength (MPa) |
|---|---|---|---|---|
| Al 6061-T6 | 2.71 | 69.04 | 313.1 | 259.2 |

## *Finite element method*

Finite Element Analysis (FEA) utilizing the Finite Element Method (FEM) is a powerful engineering tool, and when complemented with software like Ansys, it offers numerous advantages in the design and analysis of structures and components. Firstly, the accuracy of FEA is a standout feature. Ansys employs advanced algorithms that can simulate complex physical behaviours, allowing engineers to predict how a structure will respond to various loads and environmental conditions with high precision. This capability is invaluable in optimizing designs, identifying potential weaknesses, and ensuring that the final product meets performance and safety requirements.

Secondly, the versatility of Ansys in handling a wide range of engineering problems is noteworthy. Whether it's structural analysis, thermal analysis, fluid dynamics, or coupled-field problems, Ansys provides a comprehensive platform. Engineers can simulate various scenarios and study the interaction between different physical phenomena, offering a holistic understanding of the system under investigation. This versatility makes Ansys a preferred choice across diverse industries, from aerospace to automotive and beyond.

Lastly, the efficiency gained through FEA and Ansys cannot be overstated. Traditional prototyping and testing methods can be time-consuming and expensive. With FEA, engineers can iterate through design changes rapidly in the virtual environment, reducing the need for physical prototypes. This speeds up the process of developing a product while simultaneously cutting costs. The ability to identify and address potential issues early in the design phase enhances overall project efficiency and success. In summary, the combination of the Finite Element Method and Ansys software provides engineers with a robust and efficient solution for addressing complex engineering challenges across various industries.

The FEM procedure allows the continuum to be discretized into a limited number of parts (elements) and emphasizes that the continuous domain's characteristics can be estimated by assembling the same properties of discrete elements per node [19,20]. This process is known as discretization. The values at nodes are established through polynomial interpolation using the computational matrix approach [21]. The precision of the outcomes relies on discretization, the accuracy of the presumed interpolation form, and the precision of the computational solution method. The popularity of the Finite Element Method (FEM) stems from its capability to model a wide range of numerical problems, irrespective of geometry, boundary conditions, and loading.

Figure 1 depicts a rocket motor test stand design with a length of 1200 mm, a width of 600 mm, a height of 330 mm, and an internal diameter of the test stand measuring 200 mm.

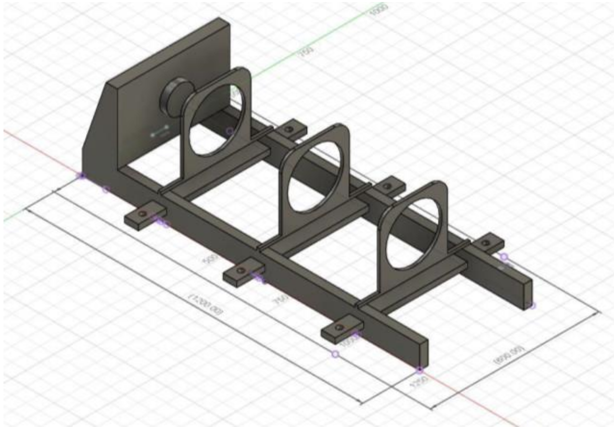

Figure 1. The rocket motor test stand design with a length of 1200 mm, a width of 600 mm, a height of 330 mm, and an internal diameter of the test stand measuring 200 mm

In Figure 2, the boundary conditions of the finite element analysis are vividly depicted, showcasing the presence of six fixed supports on the left and loading conditions on the right, with a force magnitude of 10,000 N. This visual representation offers a clear insight into the structural constraints and applied forces essential for the analysis. Complementing this visual representation, Table 2 furnishes comprehensive details regarding the assumptions and parameters incorporated in the finite element analysis conducted through Ansys Workbench. These combined visuals and data serve as a foundational reference for understanding the setup and key variables considered in the analytical framework.

Table 2. The assumptions made in the Finite Element Method (FEM) utilizing Ansys Workbench software

| Parameters | Value |
|---|---|
| Variation of thrust | 10,000; 12,000; 14,000, and 16,000 N |
| Element size | 6 mm |
| Number of nodes | 109581 |
| Number of elements | 57869 |
| Safety factor | Based on yield strength |
| Loading type | Fully reserved |
| Analysis type | Stress life |
| Mean stress theory | Gerber |
| Design life | $10^6$ cycles |

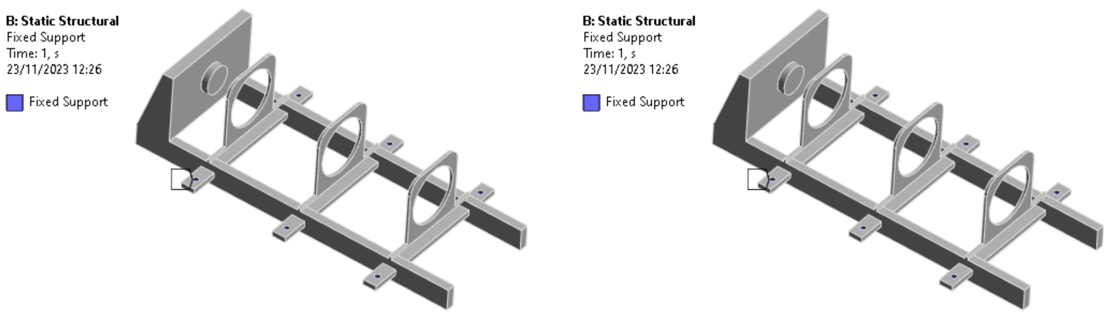


Figure 2. The six fixed support (left) and loading conditions with a force of 10,000 N (right)

## Result and Discussion

Figure 3, situated in the top-left corner, illustrates the results of the simulation concerning von Mises stress in a rocket motor test stand exposed to a thrust of 10,000 N. The highest recorded von Mises stress stands at 93.01 MPa, a value below the yield strength of Aluminium 6061-T6, which is 259.2 MPa. This observation implies that, during the initial cycle, the structural component of the rocket motor test stand is not susceptible to failure. The simulation outcomes provide a reassuring indication of the stand's structural integrity, as the stress levels remain within the material's capacity to withstand mechanical loads without permanent deformation or failure. Therefore, based on this analysis, the rocket motor test stand is deemed structurally sound and capable of withstanding the applied thrust without compromising its integrity.

Deformation in structures refers to the alteration of the shape or dimensions of an object due to external loads or forces acting upon it. This phenomenon can occur in various types of structures, including buildings, bridges, and vehicles. During deformation, an object may experience changes in length, width, or even its overall shape, which can be either temporary or permanent. A profound understanding of deformation is crucial in structural engineering as it can impact the performance and reliability of a structure. Deformation analysis helps engineers design structures that can efficiently withstand given loads, ensuring safety and structural integrity in various situations. The maximum deformation observed in this investigation is relatively small, specifically 1.11 mm, as illustrated in Figure 3 (top right).

The safety factor, a critical parameter for evaluating the safety of a component or structure based on its minimally utilized dimensions, is meticulously determined through the Ansys Workbench platform. Calculated as the yield strength of the material divided by the maximum von Mises stress, the minimum safety factor provides a key insight into the structural robustness. A safety factor below 1 would signify a permanent failure in the design, as per established engineering principles. In the case of rocket motor test stands subjected to a thrust of 10,000 N, the design proves to be secure, with a minimum safety factor of 2.79, as illustrated in Figure 3 at the bottom. These safety factor values comfortably exceed the industry standards for components facing dynamic loads, typically mandating a minimum safety factor of 2, reinforcing the reliability and strength of the design under applied stresses [22].

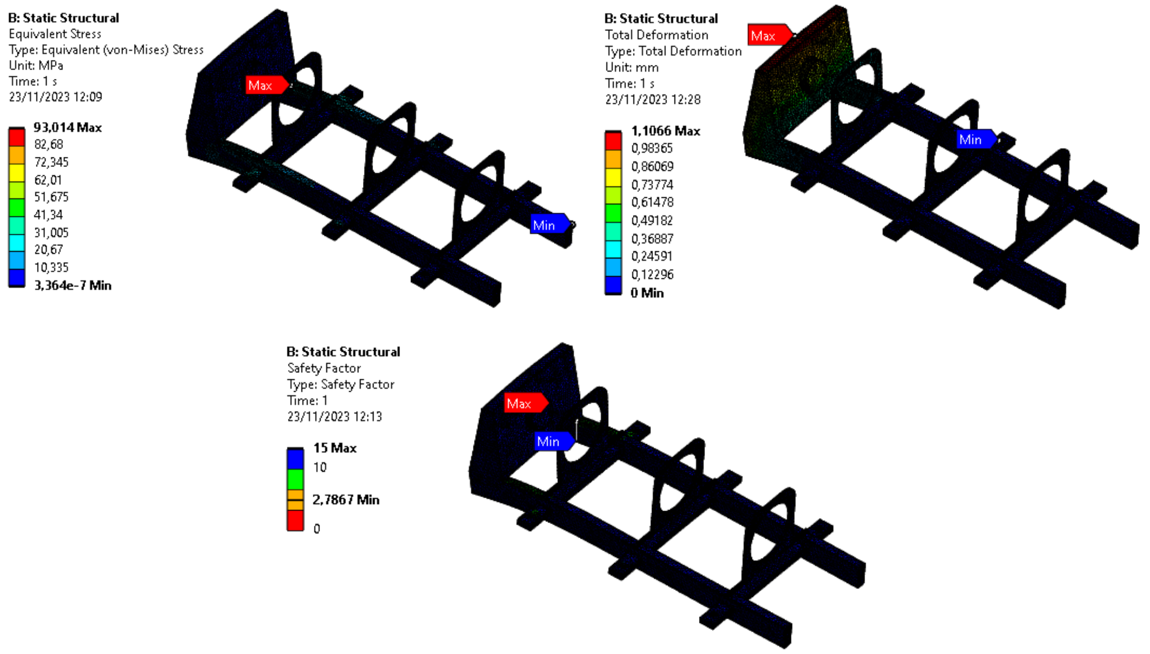


Figure 3. Static stress analysis with 10,000 N thrust variation: von Mises stress (top left), deformation (top right), and safety factor (bottom)

Table 3 provides a comprehensive depiction of how different thrust levels affect the maximum von Mises stress in the rocket motor test stand. The outcomes of static stress analysis unveil a discernible pattern: heightened thrust corresponds to an escalation in both the maximum von Mises stress and deformation within the structure. This observed relationship is inversely proportional to the safety factor, indicating that as the applied thrust increases, the safety factor for the rocket motor test stand proportionally decreases. This insight is pivotal for understanding the structural behaviour under varying operational conditions, as it emphasizes the need for meticulous consideration of safety factors in the design phase, particularly in scenarios where the thrust is anticipated to fluctuate. The correlation between thrust, von Mises stress, and safety factors elucidated by these findings contributes valuable information for optimizing the design and ensuring the structural integrity of the rocket motor test stand across a spectrum of operating conditions.

Table 3. Impact of thrust variations on the static stress of the rocket motor test stand

| Thrust (N) | Maximum von Mises stress (MPa) | Deformation (mm) | Safety factor |
|---|---|---|---|
| 10,000 | 93.01 | 1.11 | 2.79 |
| 12,000 | 111.62 | 1.33 | 2.32 |
| 14,000 | 130.22 | 1.55 | 2.00 |
| 16,000 | 148.82 | 1.77 | 1.74 |

In the realm of static stress analysis, the material remains structurally sound as long as the maximum von Mises stress remains below the yield strength of the material. However, this principle does not necessarily apply when considering fatigue life analysis. Unlike static stress analysis, fatigue analysis introduces the possibility of material failure even if the maximum von Mises stress is below the material's yield strength. This unique failure scenario is attributed to fatigue, a phenomenon induced by prolonged exposure to repeated loads. Many of these failures are associated with fluctuations induced by compressive stress within the material. The fatigue process typically unfolds in stages, commencing with an initial crack, followed by crack propagation, ultimately leading to the final failure of the material. Understanding these nuanced aspects of material behaviour is crucial for designing structures that can withstand the challenges posed by fatigue-induced failures over extended periods.

The prediction of fatigue life in this study utilizes the Gerber Mean Stress theory, an extension of the Goodman Mean Stress theory because the material used is ductile, namely Aluminium 6061-T6 [23,24]. This theory is employed in engineering to forecast material failure under cyclic loading, specifically focusing on the influence of mean stress, the average stress level during a loading cycle, on material fatigue life. The theory calculates an equivalent stress by combining alternating stress and mean stress, comparing it to the material's endurance limit. If the equivalent stress is below the endurance limit, infinite fatigue life is predicted; otherwise, the theory estimates the number of cycles to failure. This approach acknowledges the impact of mean stress on fatigue behaviour, enhancing predictions in conditions involving both cyclic and mean stresses. The Gerber Mean Stress theory proves particularly valuable in assessing the fatigue resistance of materials and components subjected to variable loading in various engineering applications.

Illustrated in Figure 4, the rocket motor test stand frame showcases a noteworthy minimum fatigue life of 37.44 million cycles in response to a thrust variation of 10,000 N. This revelation underscores the remarkable endurance capacity of the rocket motor test stand, capable of sustaining loads for a substantial duration of at least 37.44 million cycles. Moreover, this endurance is accompanied by a commendable minimum safety factor of 1.44, reaffirming the structural integrity and reliability of the test stand under the specified thrust conditions. These findings are instrumental in validating the robustness of the design, providing crucial insights into the structural performance and fatigue resistance of the rocket motor test stand over an extended operational lifespan.

Table 4 provides a comprehensive depiction of how varying levels of thrust impact the fatigue life prediction of the rocket motor test stand. The data reveals a clear correlation: increased thrust corresponds to a notable decrease in the predicted fatigue life and safety factor of the structure. Particularly, at a thrust of 16,000 N, the rocket motor test stand falls short of achieving a life expectancy of 1 million cycles, marking a critical threshold. These findings underscore the sensitivity of the test stand's fatigue life to variations in applied thrust, emphasizing the need for precise considerations in design and operational planning. The insights garnered from this analysis are crucial for engineers, as they navigate the delicate balance between optimizing performance and ensuring the structural integrity of the rocket motor test stand under diverse operational conditions.

Table 4. Impact of thrust variations on the prediction of fatigue life for the rocket motor test stand

| Thrust (N) | Fatigue life prediction (million cycles) | Safety factor |
|---|---|---|
| 10,000 | 37.44 | 1.44 |
| 12,000 | 4.52 | 1.20 |
| 14,000 | 1.20 | 1.02 |
| 16,000 | 0.46 | 0.90 |

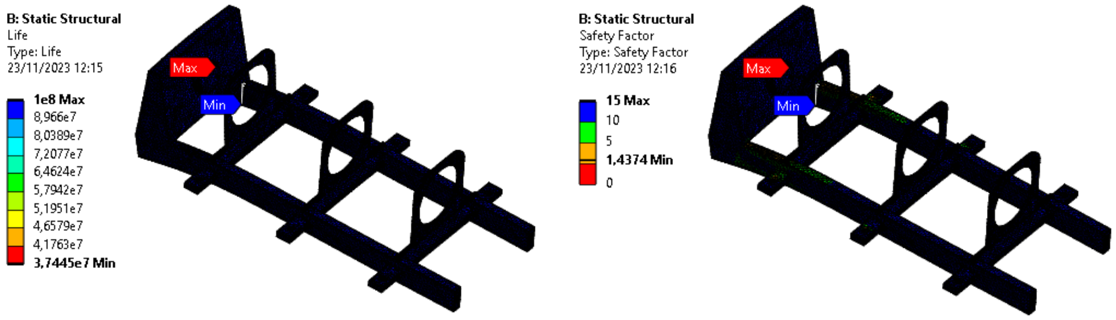


Figure 4. Prediction of fatigue life (left) and safety factor (right) for rocket motor test stand with 10,000 n thrust variation

## Conclusion

The findings from the static stress analysis indicate that as thrust increases, both the maximum von Mises stress and deformation also increase. This relationship is inversely proportional to the safety factor, meaning that with greater thrust, the safety factor of the rocket motor test stand decreases. Similarly, in the fatigue simulation results, higher thrust is associated with a reduced prediction of fatigue life and a lower safety factor. Specifically, at 16,000 N thrust, the rocket motor test stand fails to achieve a life of 1 million cycles.

## Acknowledgement

The author expresses gratitude to the Indonesian National Research and Innovation Agency (BRIN) for their generous support in facilitating this research. Their contribution has been instrumental in the successful execution of the study.

## References

[1] Summers, M. H. & Villarreal, J. K. Small - Scale Hybrid Rocket Test Stand and Characterization of Swirl Injectors. 1–13 (2013).
[2] Ortiz, L. et al. Development of a Mobile Rocket Engine Test Stand ( MRETS ). 1–17 (2018). doi:10.2514/6.2018-4600
[3] Jain, U., Shukla, H., Kapoor, S., Pandey, A. & Nirwal, H. Design and analysis of 2-axis rocket motor stand for thrust vectoring. in AIAA Propulsion and Energy 2020 Forum 1–9 (2020). doi:10.2514/6.2020-3920
[4] Prochnicki, P., Fessl, J., Moruzzi, M., Perry, E. & Targonski, J. Hydra : Development of a Liquid Rocket Engine Test Stand and Feed System. 1–20 (2018). doi:10.2514/6.2018-4601
[5] Schultz, L. et al. Design of Torsional Test Stand for Micro-Newton Force Detection. 1–14 (2018). doi:10.2514/6.2018-3737
[6] Moruzzi, M. & Fessl, J. Liquid rocket engine component water-flow test stand. in 2018 Joint

Propulsion Conference 1–18 (2018). doi:10.2514/6.2018-4599
[7] Wibawa, L. A. N. Static Stress Analysis and Fatigue Life Prediction of Rocket Motor Test Stand Using Numerical Simulation. R.E.M. (Rekayasa Energi Manufaktur) J. 6, 9–13 (2021).
[8] Mickels, C. et al. Project atlas: A mobile universal rocket engine test stand. in AIAA Scitech 2019 Forum 1–8 (2019). doi:10.2514/6.2019-1938
[9] Thomas, J. C. et al. Design and Characterization of a Lab-Scale Hybrid Rocket Test Stand. in 52nd AIAA/SAE/ASEE Joint Propulsion Conference 1–13 (2016). doi:10.2514/6.2016-4965
[10] Brimhall, Z. N., Divitotawela, N., Atkinson, J. P., Kirk, D. R. & Peebles, H. G. Design and validation of a six degree of freedom rocket motor test stand. in 44th AIAA/ASME/SAE/ASEE Joint Propulsion Conference and Exhibit (2008). doi:10.2514/6.2008-5051
[11] Brimhall, Z. N. et al. Design of a Novel Six Degree of Freedom Solid Rocket Motor Test Stand. in 43rd AIAA/ASME/SAE/ASEE Joint Propulsion Conference & Exhibit 1–7 (2007).
[12] Hansen, J. J. et al. Student design of a bipropellant liquid rocket engine and associated infrastructure. AIAA Propuls. Energy 2020 Forum 1–36 (2020). doi:10.2514/6.2020-3918
[13] Figueroa, F. & Schmalzel, J. Integrated System Health Management : Pilot Operational Implementation in a Rocket Engine Test Stand. AIAA Infotech@ Aerosp. 2010 1–14 (2010).
[14] Rezende, R. N. et al. Designing a thrust vector test stand for the TurboRocket. AIAA Propuls. Energy Forum, 2021 (2021). doi:10.2514/6.2021-3350
[15] Shukla, H., Jain, U. & Kumar, D. Preliminary Design Approach for Sub-Scale Rocket Motor Thrust Stand. in Recent Advances in Mechanical Engineering (eds. Narendranth, S., Mukunda, P. G. & Saha, U. K.) 1–17 (Springer Nature Singapore, 2023).
[16] Bouziane, M., Bertoldi, A. E. M., Milova, P., Hendrick, P. & Lefebvre, M. Development and testing of a lab-scale test-bench for hybrid rocket motors. 15th Int. Conf. Sp. Oper. 2018 (2018). doi:10.2514/6.2018-2722
[17] Wibawa, L. A. N., Diharjo, K., Raharjo, W. W. & Jihad, B. H. Stress Analysis of Thick-Walled Cylinder for Rocket Motor Case under Internal Pressure. J. Adv. Res. Fluid Mech. Therm. Sci. 70, 106–115 (2020).
[18] Wibawa, L. A. N., Diharjo, K., Raharjo, W. & Jihad, B. H. The Effect of Fillet Radius and Length of The Thick-Walled Cylinder on Von Mises Stress and Safety Factor for Rocket Motor Case. AIP Conf. Proc. 2296, (2020).
[19] Wibawa, L. A. N. & Tuswan. Lightweight optimization design of thin-walled cylindrical rocket motor tube using FEA. AIP Conf. Proc. 2590, (2023).
[20] Wibawa, L. A. N. & Setiadi. The effect of load variations and thread types on the joint strength of the rocket cap and tube using finite element method. *AIP Conf. Proc.* **2590**, (2023).
[21] Wibawa, L. A. N. & Tuswan. Effect of cylinder length on the ratio of safety factor and weight of rocket motor tube using thin-walled cylinder. AIP Conf. Proc. 2590, (2023).
[22] Dobrovolsky, V. & Zablonsky, K. Machine elements : a textbook. (Peace Publisher, 1978).
[23] Wibawa, L. A. N. Effect of Fillet Radius of UAV Main Landing Gear on Static Stress and Fatigue Life using Finite Element Method. J. Phys. Conf. Ser. 1811, (2021).
[24] Wibawa, L. A. N. Effect of Bolt Hole Size on Static Stress and Fatigue Life of UAV Main Landing Gear Using Numerical Simulation. J. Phys. Conf. Ser. 1811, (2021).